Applied Catalysis A: General 342 (2008) 150–158

Contents lists available at ScienceDirect

Applied Catalysis A: General

journal homepage: www.elsevier.com/locate/apcata

# Original carbon-based honeycomb monoliths as support of Cu or Mn catalysts for low-temperature SCR of NO: Effects of preparation variables

Mohamed Ouzzine [a], Gustavo A. Cifredo [b], José M. Gatica [b,*], Sanae Harti [a], Tarik Chafik [a], Hilario Vidal [b]

[a] Laboratoire de Génie Chimique et Valorisation des Ressources, Faculté des Sciences et Techniques, Université Abdelmalek Essaadi, B.P. 416 Tangier, Morocco
[b] Departamento C.M., I.M. y Química Inorgánica, Universidad de Cádiz, Puerto Real 11510, Spain

ARTICLE INFO

*Article history:*
Received 8 February 2008
Received in revised form 7 March 2008
Accepted 11 March 2008
Available online 19 March 2008

*Keywords:*
Carbon monoliths
Preparation method
NO abatement
SCR with $NH_3$
Copper catalysts

ABSTRACT

A series of catalysts consisting in Cu or Mn supported on lab-scale carbon-based honeycomb monoliths, which have been previously prepared following an original methodology, have been investigated in the low-temperature selective catalytic reduction of NO with $NH_3$. Special attention has been paid to the effect of changing different preparative variables for the incorporation of the active phase: way of introducing the metal, concentration of the precursor solution and time of contact with the monoliths in the case of impregnation, use or not of a chemical pre-treatment of the support, and the final drying procedure. Complementary techniques employed for the chemical, textural and structural characterisation have revealed significant differences between the catalysts depending on their preparative procedure.



## 1. Introduction

Carbon, especially upon activation, is traditionally one of the most commonly employed materials for adsorption applications due to its porosity properties [1]. Nevertheless, it is seldom used as catalytic support of honeycomb monoliths type [2], as compared to powder, granules, spheres, extrudates, pellets and tablets. Thus, although a monolithic reactor would offer clear advantages in relation to a conventional packed bed such as less pressure drop and easier handling [3,4], carbon rheological properties render difficult its extrusion [5].

In previous works however we demonstrated that, with the use of appropriate additives, obtaining carbon-based monoliths is not only possible but also easily controllable following methodologies originally developed for ceramic materials [6–8] that allow optimizing the composition of the carbonaceous dough in order to be extruded. Further we showed that the resulting monoliths were potential candidates as VOCs adsorbents after being activated [8]. The present work aims to investigate the application of the obtained carbon monoliths as support of metal active phases for environmental catalysis applications. In particular, different samples constituted by copper or manganese supported on carbon-based lab-scale honeycomb monoliths have been prepared for the selective catalytic reduction (SCR) of NO with ammonia. This reaction is one of the favourite applications of monoliths for gas phase catalysis [9,10]. Besides this, the combination of carbon as material support and metal oxides (V, Fe or Mn, and even Cu although much less investigated) as active phase has been recently proposed for the NO-SCR as interesting alternatives respect the commercial $V_2O_5$-$WO_3$/$TiO_2$ [11]. The reason is that carbon-based catalysts show high activity around 200 °C instead of the usual operation conditions (300–400 °C) allowing to be placed in the downstream where there is a less aggressive atmosphere concerning particles concentration and $SO_2$ content. The use of carbon in the formulation for NO-SCR catalysts have been previously investigated but in the form of carbon-coated cordierite monoliths [12].

The main scope at this stage was to study the influence of the metal phase incorporation procedure on its final state besides the texture and structure of the catalysts as all these properties are crucial for the application of any heterogeneous catalyst [13]. In particular, it is well known that in order to obtain a good distribution besides an acceptable dispersion of the active phase great care must be taken in the catalysts preparation [14], particularly in the monolithic design in which the amount of active phase related to the total volume of catalyst is much lower compared to powder beds or extrudates [9]. For this reason the following preparative variables were investigated: (1) the way of introducing the metal [15]; (2) the

* Corresponding author at: Tel.: +34 956 016344; fax: +34 956 016288.
*E-mail address:* josemanuel.gatica@uca.es (J.M. Gatica).

0926-860X/$ – see front matter © 2008 Elsevier B.V. All rights reserved.
doi:10.1016/j.apcata.2008.03.014

concentration of the precursor solution in those catalysts prepared via impregnation technique; (3) the time of contact between the monoliths and such solution; (4) the use or not of an acid or acid/basic chemical pre-treatment of the support [16]; (5) the final drying method, conventional or microwaves assisted [17].

To the best of our knowledge no similar work is found in literature, dealing with the study of the effect of the preparation method on metal supported on carbon-based monoliths, especially with a wide variety of complementary characterisation techniques as here employed, that give information concerning composition, texture, chemical behaviour and particularly fine details of the materials structure, being only available references related with washcoated cordierites as support [17,18].

## 2. Experimental

### 2.1. Materials

The carbon-based honeycomb monoliths used in the present work were prepared from a medium volatile bituminous coal provided by the National Institute of Carbon in Spain, whose composition was 30 wt% of volatile and less than 6 wt% of ashes, and 75 vol% of vitrinite phase concerning its maceral composition. Its extrusion was achieved according to a previously reported methodology [6,7] using the following additives: 9.5% silicate clay (ARGI-2000 from VICAR, S.A.), 2.5% glycerine, 1.9% methylcellulose, and 0.3% aluminium phosphate dissolved in *o*-phosphoric acid (weight percentages referred to the extrudable paste excluding water). The plastic properties of the extrudable dough were liquid limit = 47% and plasticity index = 24%, parameters defined and measured according to previous references [19]. After extrusion the green monoliths were dried at 80 °C overnight and submitted to preoxidation (air, 250 °C, 24 h), carbonization (Ar, 840 °C, 1 h) and finally, activation ($H_2O$, 250 Torr/Ar, 860 °C up to a burn-off degree of 15%). The resulting honeycomb monoliths had the following geometric characteristics: square section, 13.7 cells/cm$^2$, 0.08 cm of wall thickness, a geometric surface area of 10.4 cm$^2$/cm$^3$ with 49 % open frontal area.

Regarding the metal precursors two nitrate salts were employed: $Cu(NO_3)_2{\cdot}3H_2O$ from PANREAC, S.A. and $Mn(NO_3)_2{\cdot}4H_2O$ from Sigma–Aldrich with 99% and 98.5% of purity, respectively.

### 2.2. Catalyst preparation

Three different preparation methods have been used for metal introduction on carbon-based honeycomb monoliths: (1) impregnation with the precursor solution, (2) integration in the paste before the extrusion step, and (3) homogeneous deposition-precipitation from urea decomposition. In the first case the concentration of the precursor solution was adjusted to 1 or 2 M, and different times of contact with the monolith were tested: 30, 60, and 90 min. In some cases a pre-treatment of the support with a 65 wt%. $HNO_3$ solution during 1 h at 60 °C followed or not by an additional treatment with a 0.05-M NaOH solution for 1 h at room temperature was applied before the metal impregnation. The resulting impregnated samples were dried either conventionally (in an oven at 90 °C overnight) or using microwaves (500 W, 1 min). For the sake of clarity the following nomenclature has been adopted to identify each sample according to its preparation method: first the metal symbol, then the initials "int" or "dp", if the catalyst is prepared by integration or deposition-precipitation, respectively, or three numbers in the case of impregnation which denote consecutively the lack of support pre-treatment (0) or its existence (acid, 1 or acid/basic, 2), the precursor solution concentration and the contact time; finally, a letter (conventional, C or microwaves assisted, M) which indicates the drying method, followed by an asterisk in those samples in which there is no final metal activation. As an example, Cu 0.1.30.M would refer to a copper catalyst prepared by impregnation of a non pre-treated monolith with a 1-M nitrate precursor solution during 30 min which has been finally dried using microwaves and subjected to final activation of the metal according to the procedure further indicated.

The Cu int catalyst was prepared adding 15 ml of a 4-M precursor solution in three steps to 50 mg of the extrudable carbonaceous paste. After extrusion and drying overnight at 100 °C under synthetic air flow, the resulting monolith was calcined in Ar at 400 °C for 1 h. The Cu dp catalyst was prepared by immersing the carbon-based monolith support in a mixture of 10 ml of a 0.1-M precursor solution and 15 ml of a 1-M urea solution and heating at 90 °C during 10 h. Afterwards the monolith was dried in an oven at 90 °C overnight.

### 2.3. Characterisation techniques

Textural characterisation has been carried out by physical adsorption of $N_2$ at −196 °C in a Micromeritics ASAP 2020 using its software utilities for the data reduction. Scanning Electron Microscope (SEM) images and EDS data have been obtained using a Quanta 200 scanning electron microscope (Philips) equipped with a Phoenix Microanalysis system using a nominal resolution of 3 nm. Induced coupled plasma spectroscopy (ICP) analysis of the chemical composition was performed using an IRIS Intrepid HR instrument. X-ray diffraction (XRD) was carried out at room temperature using a Bruker D8-500 powder diffractometer operating with Cu Kα radiation and the Rietveld analysis of the data was performed using the Fullproof program [20]. Thermogravimetric analysis was carried out both under air or He flow with a TA thermobalance, model SDT Q600, using 25 mg of crushed samples and a heating rate of 10 °C/min. Complementary temperature programmed desorption (TPD), reduction (TPR) and oxidation (TPO) experiments were performed employing a Thermostar QMS 200 (Pfeiffer) mass spectrometer with a 60 ml/min flow of He, $H_2$-5% or $O_2$-5%, respectively, and using also milled pieces of monoliths (50 mg) and 10 °C/min as heating rate.

### 2.4. Catalytic activity tests

The evaluation of the catalysts activity was performed in a stainless steel continuous flow reactor of 1.35-cm internal diameter and an internal sample holder with allows preventing the gases from bypassing the monolith. A $0.90 \pm 0.05$-cm edge square section and 4-cm long monolith was used for each test and a pre-treatment consisting on heating at 250 °C in a 120-ml/min He flow for 1 h was applied before running the experiments, according to the below described study, with exception of Cu int for which the temperature chosen was 400 °C. The experiments consisted in heating the sample under the reactant mixture up to 500 °C using a rate of 5 °C/min. Reaction conditions were selected considering previous similar experiences of other authors with lab-scale monoliths [21–23]. The gas composition was 3000 ppm NO, 6000 ppm $NH_3$, 2 vol% $O_2$ balanced by He and $N_2$. The total flow rate was 345 ml/min, which corresponds to a GHSV of 6390 h$^{-1}$. NO concentration in the outlet gases were continuously measured in a NGA 2000 Fisher Rosemount CLD analyzer module using a chemiluminiscence detector.

## 3. Results and discussion

### 3.1. Thermal analysis

Prior to any other study, thermal analysis of the metal-containing monoliths was performed in order to know their

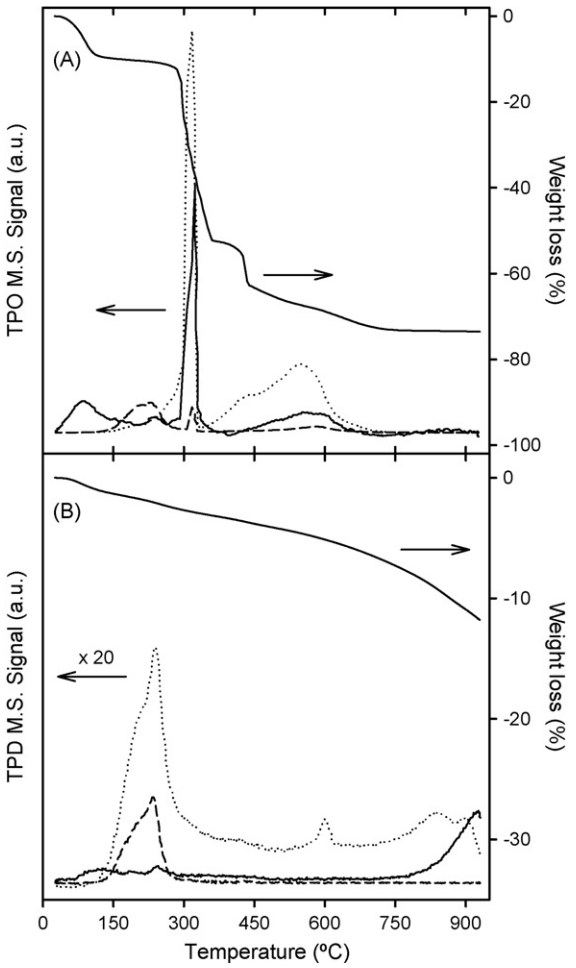


**Fig. 1.** Study by (A) TGA (air) and TPO (5% $O_2$) and (B) TGA (He) and TPD (He) of Cu 0.1.90.C*. In the case of TPO and TPD the traces correspond to (–) water, *m*/*e* 18; (- - -) nitrogen oxides, *m*/*e* 30; (···) carbon dioxide, *m*/*e* 44 signals.

stability and to establish the most appropriate pre-treatment leading to metal phase activation. Fig. 1 shows the TGA curves recorded both under air (A) and inert gas (B), and the most significant traces recorded during TPD and TPO experiments of a Cu 0.1.90.C* monolith, which has been selected as representative sample, given the fact the similar results obtained with other studied impregnated catalysts. As shown in Fig. 1A, the TGA diagram obtained under air and the *m*/*e* 44 signal of the TPO experiment suggest that, in the presence of $O_2$, approaching a temperature as low as 300 °C implies already a significant loss of material. Moreover further weight loss is detected up to 700 °C. On the contrary, flowing inert gas at 250 °C for 1 h can be an appropriate activation treatment to decompose most of the metal precursor (see *m*/*e* 30 evolution corresponding to nitrate decomposition via nitrogen oxides) without intense burning of the carbon support (Fig. 1B). Although not shown, in a parallel study of the monolith support without metal, $NO_x$ were not detected when the sample was heated in inert gas. Notice that although carbon support is also being lost during heating in inert gas (observe *m*/*e* 44 in Fig. 1B) this process is much less significant as the TGA relative intensity denotes. Furthermore, the above treatment in He does not presumably induce undesirable sintering effects on the metal phase as other references in literature on Cu-supported catalysts suggest [24]. In addition, behaviour of manganese-supported catalysts investigated appeared to be very similar showing even a slight anticipation of the precursor decomposition

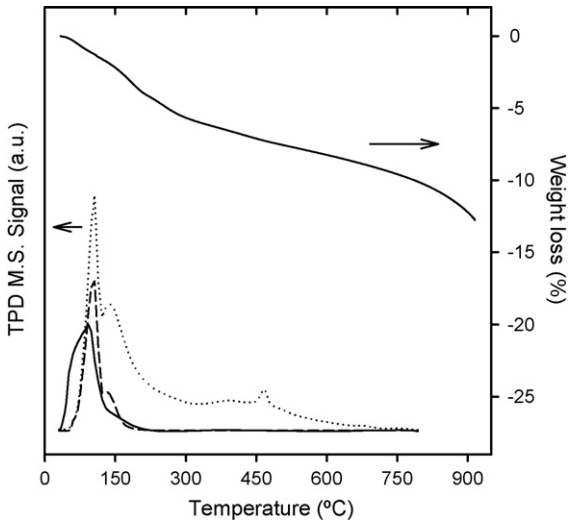


**Fig. 2.** Study by TGA (He) and TPD (He) of Mn 0.1.60.C*. In the case of TPD the traces correspond to (–) water, *m*/*e* 18; (- - -) nitrogen oxides, *m*/*e* 30; (···) carbon dioxide, *m*/*e* 44 signals.

(Fig. 2). Therefore, unless indicated (samples with the asterisk mark) this treatment (He, 250 °C, 1 h) was systematically adopted for all catalysts prepared by contact of the carbon-based monoliths with a metal precursor solution, including the so-called "dp" sample after the drying step. The case of the Cu int catalyst is special as metal is included along with the additives necessary for carbon extrusion. TGA and TPD studies (results not shown) suggested the treatment previously indicated in Section 2 for this sample.

### 3.2. Metal loading analysis

Results obtained by ICP analysis for most of the catalysts investigated are summarized in Table 1 and deserve several comments. First it can be observed that the amount of metal introduced in the impregnated samples ranges approximately from 2 to 5 wt.%. Among the copper catalysts it is interesting to notice, however, the clearly lowest value obtained for Cu 0.1.30.C. On this regard, it should be considered that in this sample, as other authors have previously observed on different monolith supports [17], heterogeneity of the metal distribution as consequence of

**Table 1**
Textural data obtained by means of $N_2$ physisorption at −196 °C and metal content of the samples as determined by induced coupled plasma spectroscopy (ICP)

| Sample | Metal (wt. %) | Textural data | |
|---|---|---|---|
| | | BET surface area ($m^2$/g) | Micropore volume (ml/g)[a] |
| Cu 0.1.30.C | 2.16 ± 0.07 | 200 | 0.090 |
| Cu 0.1.30.M | 4.73 ± 0.10 | 451 | 0.170 |
| Cu 0.1.30.M* | 5.10 ± 0.10 | 474 | 0.141 |
| Cu 1.1.30.C | 2.73 ± 0.10 | 330 | 0.149 |
| Cu 1.1.30.M | 5.39 ± 0.11 | 355 | 0.153 |
| Cu 1.1.30.M* | 5.44 ± 0.11 | – | – |
| Cu 0.1.90.C | 4.01 ± 0.10 | – | – |
| Cu 0.2.30.C | 3.24 ± 0.10 | – | – |
| Cu 2.1.30.C | 4.26 ± 0.10 | – | – |
| Mn 0.1.60.C | 2.13 ± 0.04 | 518 | 0.234 |
| Mn 0.1.60.C* | 1.93 ± 0.04 | – | – |
| Cu int | 9.33 ± 0.18 | 5 | 0.003 |
| Cu dp | 0.87 ± 0.02 | 310 | 0.138 |
| Cu dp* | 0.84 ± 0.02 | – | – |
| Monolith support | Not detected | 520 | 0.195 |

[a] Data estimated from *t*-plots (Harkins-Jura) analysis.

copper migration is not discarded. As a matter of fact, a simple visual observation allowed us to detect light blue stains denotative of higher metal concentration at different parts of the monoliths, especially at the borders, which therefore were avoided for the analysis.

Another interesting effect that can be rationalized through results included in Table 1 is that the support pre-treatment with $HNO_3$ does not favour the metal incorporation significantly. This can be noticed for instance comparing values obtained for Cu 0.1.30.M and Cu 1.1.30.M or for Cu 0.1.30.M* and Cu 1.1.30.M*. On the contrary, assuming that the analysis of all conventionally dried copper catalysts could be affected by the same uncertainty due to the commented problem of heterogeneity, relative comparison between Cu 2.1.30.C and Cu 1.1.30.C suggests that additional support pre-treatment with NaOH does increase the metal loading. For the same reason, it can be concluded that both the increase in the metal concentration of the precursor (Cu 0.2.30.C) and its time of contact with the monolith (Cu 0.1.90.C), as expected, favour the metal entrance. It is important to note that similar metal contents were measured for couples of samples just differing on the metal activation, a process that, considering the low metal content in all samples if compared with the support, should have a minimum effect on the final result (see Cu 1.1.30.M and Cu 1.1.30.M*, Cu 0.1.30.M and Cu 0.1.30.M*). This shows the reproducibility of the analysis performed and at the same time might be taken as indicative of a more homogeneous distribution of the metal on the catalyst support upon microwaves assisted drying. In this sense, the similarity found for the manganese samples pair, Mn 0.1.60.C and Mn 0.1.60.C*, can be related to the fact that in this case conventional drying overnight at 90 °C might be enough to decompose the nitrate as the thermal analysis suggests (recall Fig. 2) so water desorption could occur more rapidly preventing metal phase migration. Finally, note the different metal loadings attained in those catalysts prepared following other methods than impregnation, especially the Cu int sample. In this case the clearly higher metal content was intentionally sought to ensure a significant amount of metal on the monolith surface, and therefore accessible for catalysis, as most of it must remain integrated in its matrix.

### 3.3. Textural characterisation

The main results obtained from the $N_2$ adsorption studies are also collected in Table 1. This data were extracted from the recorded isotherms (not shown) which were in all cases type-I characteristic of materials having micropores, textural feature already observed in the bare carbon support [7,8]. As can be noticed, significant differences in the textural properties of the catalysts are observed depending on the preparation procedure followed. First of all, it is interesting to see how, among the impregnated catalysts, Cu 0.1.30.C is the one showing lowest value of BET surface area mainly due to a loss of both microporosity (Table 1) and mesoporosity, according to Fig. 3 which represents the incremental pore volume distribution. This could be interpreted if, for any reason, metal precursor decomposition had not been completed in this sample inducing large crystals that block the pores. In this sense, microwaves drying could help taking into account the slightly higher temperatures reached in the sample (approximately 120 °C instead of 90 °C) and explain why textural properties improve so much after its application (see Cu 0.1.30.M). Contrarily, a chemical support pre-treatment, which according to the bibliography should increase microporosity [16], seems to loose effectiveness once the metal is introduced, as denoted by the lower BET surface area and micropores volume values measured for Cu 1.1.30.C and Cu 1.1.30.M (Table 1), and the poorer

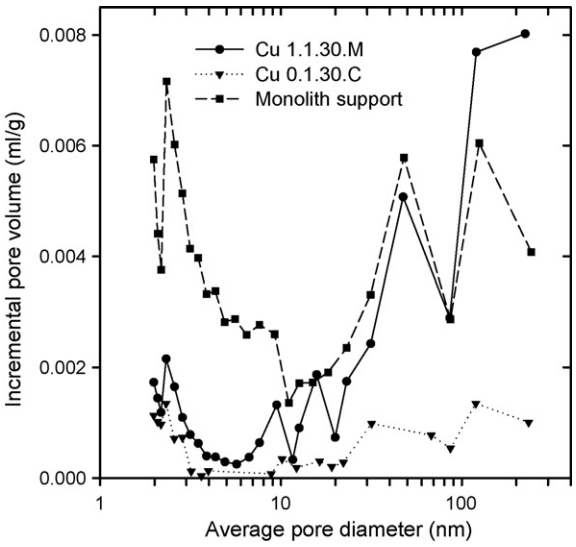


**Fig. 3.** Porosity study corresponding to the indicated samples by means of BHJ analysis of the adsorption branch of the $N_2$ isotherms (−196 °C).

mesoporosity whit regard to the starting support (Fig. 3). The use of the homogeneous deposition-precipitation method to introduce the metal (Cu dp) also leads to a worse final texture. In the case of the manganese catalyst, the metal incorporation does not seem to affect the support texture as it is the Mn 0.1.60.C sample the one exhibiting most similar surface area and microporosity respect the bare support. This suggests that similar preparation procedures (including the activation step) can lead to different final texture depending on the metal employed. Finally, the very low values of BET surface area and pore volume observed for the Cu int catalyst can be understood considering that this sample must still contain most of the additives employed for the carbon extrusion, as the metal activation treatment is insufficient to achieve their elimination from carbon pores.

### 3.4. XRD-Rietveld analysis

The use of Rietveld analysis of the collected X-ray diffraction data reveals the high complexity of the structural composition of the catalysts. As an example, Fig. 4 shows the experimental diffractogram recorded for the Cu 0.1.30.M sample along with its deconvolution into different phases as deduced by Rietveld analysis. The refinement of the analysis performed is proven by the fact that modifications in the copper lattice parameter induced by the size and shape of the metal nanoparticles have been taken in to account [25]. On the other hand, Table 2 summarizes the major metallic phases detected following data treatment for some investigated catalysts. Estimate of the average crystal size as an indication of the grade of dispersion reached by copper is also included.

The most significant result worthy of comment is that, as above proposed, the nitrate precursor species seem to be still present in the Cu 0.1.30.C catalyst indicating that the metal activation treatment applied to all samples has not been really efficient in this one. This could explain its lower BET surface area and porosity commented before as these nitrate species should be found in the surface of the carbon support. It must be pointed out that in this sample, although other metallic phases were also detected, nitrate-containing phases are majority besides having large crystal size. An explanation for the contradiction between this result and those of thermal analysis above commented which recommended the activation treatment applied could be that the latter was performed over crushed monoliths in quartz low volume reactors

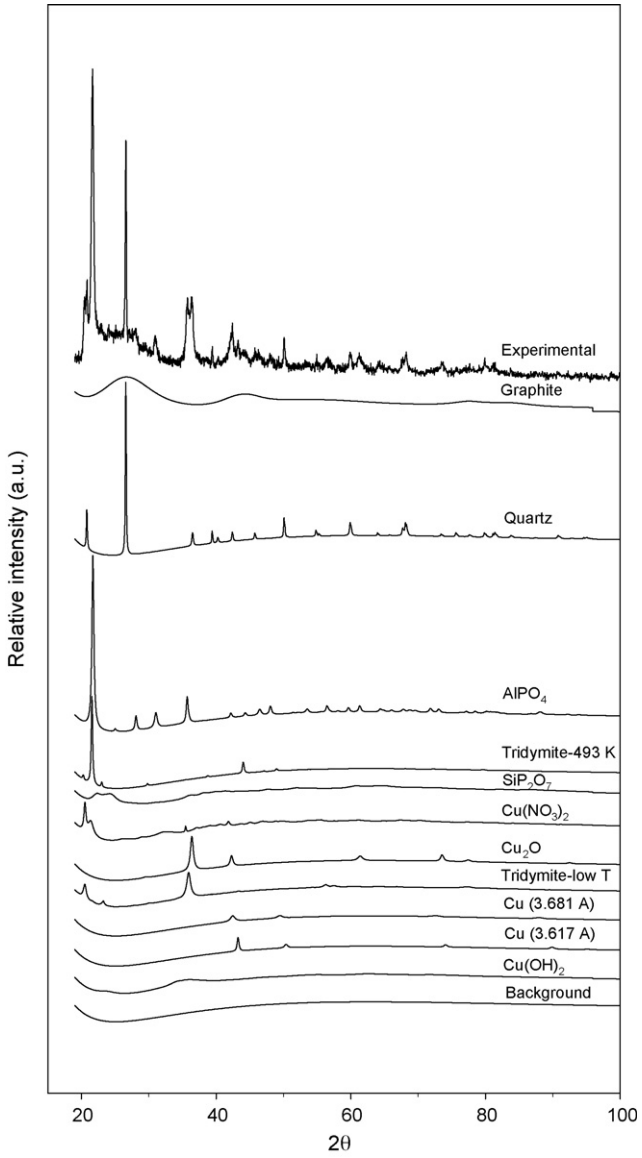


**Fig. 4.** X-ray diffractogram and Rietveld analysis of the Cu 0.1.30.M sample.

while real activation was done using reactors which allow the treatment of several monoliths at the same time, i.e. under experimental conditions which might imply mass and/or heat transfer problems and reduce the expected effect of heating.

**Table 2**
Results of Rietveld analysis of XRD data collected on copper-supported monoliths

| Sample | Major metal phases | Average crystal size (Å) |
|---|---|---|
| Cu 0.1.30.C | $Cu_2(OH)_3NO_3$ | 580 |
| | $Cu(NO_3)_2$ | – |
| Cu 0.1.30.M | $Cu_2O$ | 259 |
| | $Cu^0$ | 377, 158 (bimodal) |
| Cu 0.1.30.M* | $Cu_2(OH)_3NO_3$ | 66 |
| Cu 1.1.30.M | $Cu_2O$ | 252 |
| | $Cu^0$ | 217 |
| Cu 1.1.30.M* | $Cu_2(OH)_3NO_3$ | 34 |
| | $Cu_2O$ | 102 |
| | $Cu^0$ | 1160, 36 (bimodal) |
| Cu int | $CuHPO_4{\cdot}H_2O$ | 262 |

On the other hand, the XRD analysis suggests that microwave drying facilitates and even anticipates nitrates decomposition and leads to a better metal dispersion, also in agreement with above results. In this sense, notice that although a nitrate phase is still present in Cu 0.1.30.M*, its average crystal size has significantly diminished respect that in Cu 0.1.30.C, and this phase has disappeared in Cu 0.1.30.M. It is also remarkable that integration of copper before obtaining the monolith support seems to induce its reaction with some of the additives employed for extrusion. On this regard, notice the phosphate formation observed for the Cu int sample.

### 3.5. SEM-EDS study

The SEM technique reveals significant differences between the samples at the micron-sized level. The set of the research results obtained, a selection of which is shown in Fig. 5, might help to understand how the metal phase is supported on the monoliths. Considering that particles with bright contrast correspond to the metal phase, as confirmed by means of the EDS probe coupled with the electron microscope, notice the different aspect and bigger size of these particles in Cu 0.1.30.C in relation to Cu 0.1.30.M. It can be also noticed an intermediate look for Cu 0.1.30.M* with similar shape but much smaller grains. This suggests that decomposition of the nitrate precursor has not taken place yet in this sample, as it needs the metal activation thermal treatment, but fragmentation of its crystals must have already occurred induced by the microwaves. This observation is coherent with conclusion obtained by XRD (Table 2). It should be noticed that, according to their size, particles observation by SEM must be certainly related with aggregates of the crystals detected by XRD. So both techniques provide complementary information.

Fig. 6 illustrates the aspect presented by two other samples, Cu 1.1.30.C and Cu 2.1.30.C. These images confirm what was previously anticipated by ICP: the different effect of an acid and an acid/basic pre-treatment of the monolith before metal impregnation. While $HNO_3$ does not change significantly the support texture (see the relatively flat look similar to that previously observed for unloaded monoliths [8]) further contact with NaOH affects considerably its surface creating more roughness and porosity, apart from its chemical nature, favouring the metal incorporation.

Mapping by EDS allows getting clearer evidence of the better metal distribution for microwaves dried samples in good agreement with the XRD investigations as well as with previous studies reported for other monolithic supports [17]. Elemental mapping of copper in the Cu 0.1.30.C and Cu 0.1.30.M catalysts shown in Fig. 7 demonstrates that copper is present as large aggregates in the former while it is more evenly spread in the latter. Also remarkable, mapping of the Mn 0.1.60.C sample (also included in Fig. 7) indicates a metal distribution more similar to that observed for Cu 0.1.30.M which means that in the case of manganese catalysts it might not be necessary the use of microwaves to attain good physicochemical properties in agreement with the textural characterisation results above commented.

The EDS technique has also allowed to detect in all the monoliths the presence of minor amounts of both metallic (Al, K, Ca, Fe, Ti) and pseudo and non-metallic elements (Si, P, S) in good agreement with the presence of ashes in the starting carbon material and the use of additives for its further extrusion. The possible influence of these elements on the catalytic activity will be discussed in Section 3.7.

### 3.6. TPR–TPO investigation

For better understanding the differences observed between Cu 0.1.30.C and Cu 0.1.30.M samples, additional TPR and TPO

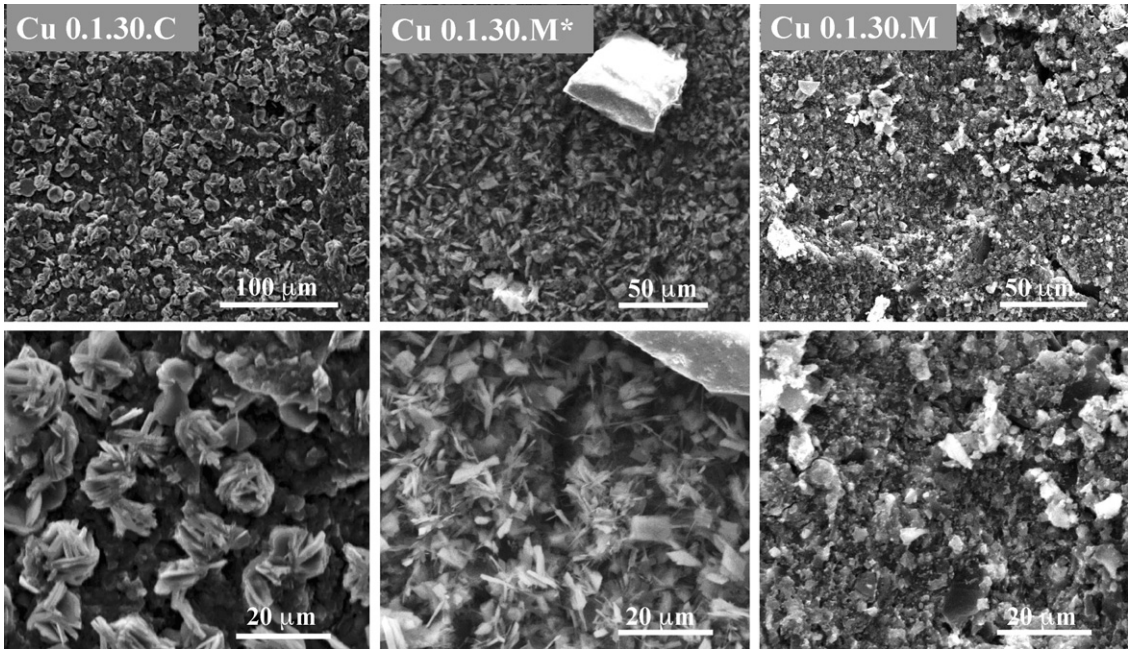


**Fig. 5.** Study by scanning electron microcospy of the drying method effect on the copper-supported monoliths investigated.

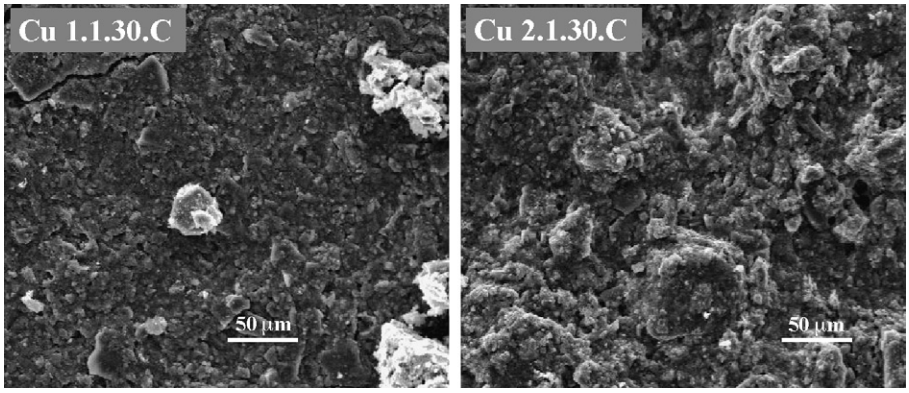


**Fig. 6.** Scanning electron micrographs of some copper-supported monoliths in which chemical treatment of the carbon was performed before metal impregnation.

experiments have been carried out regarding their particular sensitiveness to the metal phase nature. The main profiles, *m*/*e* 2 signal in the case of the TPR, corresponding to $H_2$ consumption, and *m*/*e* 30 and 32 signals in the case of TPO, that show the $NO_x$ evolution and the $O_2$ consumption respectively during the oxidation process, are presented in Figs. 8 (TPR) and 9 (TPO). For comparative purposes signals obtained in the same kind of experiments performed with monolith support only and during TPR of a CuO reference sample are also included. Notice that the single peak detected in the latter (Fig. 8, trace a) can be reasonably attributed to reduction from the 2+ oxidation state to the 0 in copper [26]. When compared with the support (trace d) the major difference given by TPR for Cu 0.1.30.C (trace c) and Cu 0.1.30.M (trace b) is observed in the range of moderate temperatures below 500 °C and might correspond to the reduction of Cu species including oxides and nitrates. In this sense, in spite of the complexity of the analysis [26], differences between traces (a) and (b) suggest the presence of $Cu_2O$ in the supported catalyst, in good agreement with Rietveld analysis of this sample which indicated the presence of Cu(I). By the other hand the TPR investigation allows to observe carbon gasification processes with parallel hydrogen consumption at the higher temperatures studied. As the analysis by TPO (Fig. 9) is concerned the study confirms that after conventional drying a significant amount of nitrates are still present. Note the peak around 250 °C of signal *m*/*e* 30 in Cu 0.1.30.C which is absent in Cu 0.1.30.M and in the bare support. In the latter *m*/*e* 30 signal at high temperature evolves from the nitrogen originally present in the carbon employed [7]. In this sense the peaks observed at medium temperatures for Cu 0.1.30.M should be interpreted as a catalytic effect of the support nitrogen oxidation induced by the activated metal phase in this sample and not proceeding from the metal precursor. It is also significant the similarity of the oxide consumption regarding carbon burning for the Cu 0.1.30.C catalyst and the monolith support which is in contrast with that of Cu 0.1.30.M which shows the beginning of this process at much lower temperature, indicating again the existence of an activated metal phase in the latter.

### 3.7. Catalytic activity measurements

Fig. 10 shows the NO conversion curves as function of the reaction temperature obtained during the SCR tests with ammonia. Oxidation to $NO_2$ was checked and not detected in the range of temperatures and gas composition here studied. This result is

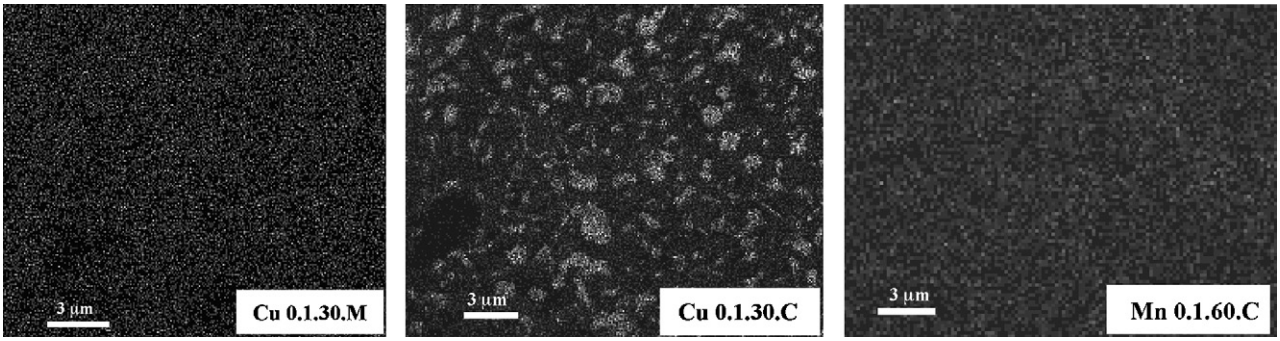


**Fig. 7.** Metal (bright spots) distribution as obtained by EDS mapping for the Cu- and Mn-supported monoliths indicated.

coherent with observations from other authors [27,28] who even in more oxidizing conditions did not find significant formation of nitrogen dioxide. The first comment that must be made is that in general the catalysts investigated exhibit high activity, especially Cu 0.1.30.C and Cu 1.1.30.C for which a conversion of 50% is attained around 200 °C (Table 3) and 90% at relatively low temperature (250 °C). This result is better than that reported in literature for other copper catalysts supported either on $SiO_2$–$Al_2O_3$ [29], $Al_2O_3$, $TiO_2$ and $SiO_2$ [30], carbon/ceramic monoliths [31], aluminosilicate monoliths [32], porous clay heterostructures [33] or modified acidic silicas [34], or for Fe-ZSM5 monolith catalysts [28], and similar to that of carbon nanotubes-supported vanadium oxides [35] and many other supported transition metal oxides [36]. Also remarkable the catalysts are thermally stable as the decrease of the activity detected at high temperature cannot be associated with a deactivation process but rather with the well-known effect due to the competition of the ammonia oxidation reaction producing NO [3]. This interpretation was checked running consecutive experiments on the same catalyst obtaining a very slightly decrease of the activity or even its increase (case of Mn 0.1.60.C) as Table 3 illustrates. In the case of Cu 0.1.30.C the catalytic performance was checked after a higher number of cycles or maintaining the sample under the reaction mixture at 270 °C for several hours, and these experiments confirmed the thermal stability commented.

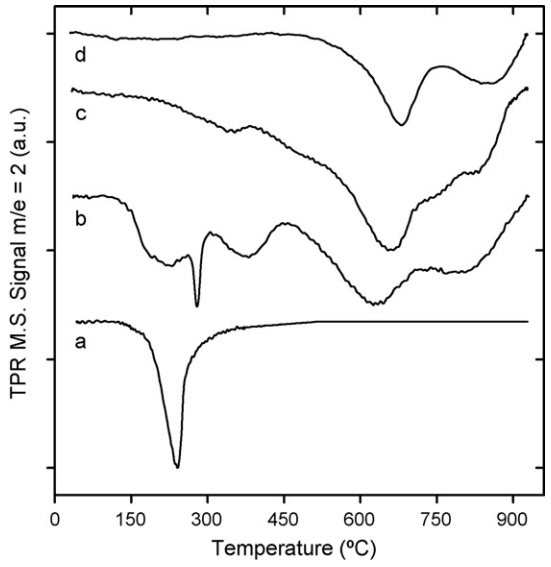


**Fig. 8.** TPR diagrams showing $H_2$ ($m/e$ 2) consumption obtained for (a) CuO, (b) Cu 0.1.30.M, (c) Cu 0.1.30.C and (d) the monolith support.

When comparison between different catalysts is made it is evident that strong differences are however observed. For instance, it is interesting to note that the Cu 0.1.30.C catalyst is in principle more active than Cu 0.1.30.M in spite of its worse metal distribution according to the EDS mapping commented above. This might be related to the different redox nature of copper in both samples, in good agreement with other authors [37] who

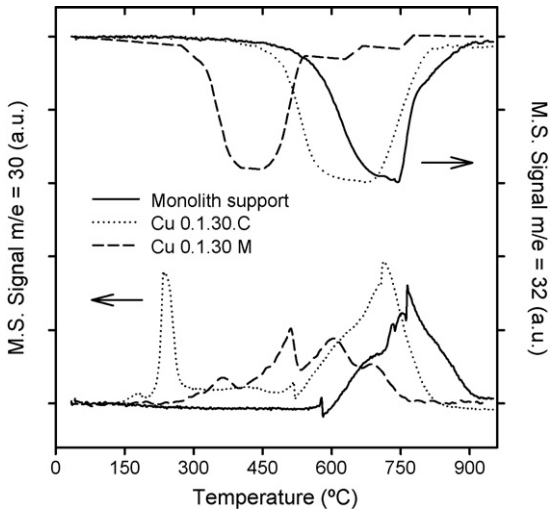


**Fig. 9.** TPO diagrams showing $O_2$ ($m/e$ 32) consumption and $NO_x$ ($m/e$ 30) evolution obtained for some copper-supported monoliths.

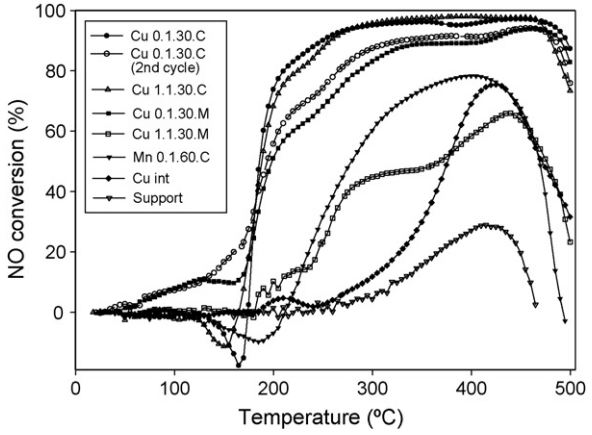


**Fig. 10.** Effect of reaction temperature on NO conversion as obtained during SCR tests with $NH_3$ (reaction conditions: GHSV: 6390 $h^{-1}$; gas inlet: 3000 ppm NO, 6000 ppm $NH_3$, 2% $O_2$ and $He/N_2$ for balance).

**Table 3**
SCR of NO results over some of the catalysts investigated using $NH_3$ as reducing agent

| Sample | First cycle | | | | Second cycle[a] | | |
|---|---|---|---|---|---|---|---|
| | W/F[b] | $T_{50}$[c] | $T_m$[d] | % NO conv. | $T_{50}$[c] | $T_m$[d] | % NO conv. |
| Cu 0.1.30.C | 0.30 | 181 | 300 | 95 | 194 | 330 | 90 |
| Cu 0.1.30.M | 0.37 | 199 | 335 | 88 | 207 | 350 | 85 |
| Cu 1.1.30.C | 0.27 | 189 | 300 | 95 | – | – | – |
| Cu 1.1.30.M | 0.09 | 368 | 440 | 66 | – | – | – |
| Cu int | 0.32 | 377 | 420 | 75 | – | – | – |
| Mn 0.1.60.C | 0.21 | 278 | 400 | 78 | 241 | 360 | 83 |
| Support | 0.16 | n.r.[e] | 415 | 29 | – | – | – |

[a] After a first run up to 500 °C the sample was cooled down to room temperature under inert gas.
[b] W/F, g s/ml.
[c] $T_{50}$, temperature at which 50% of conversion is reached.
[d] $T_m$, lowest temperature (°C) at which maximum NO conversion is reached.
[e] Not reached.

studying copper-impregnated Al–Ce-pillared clays for selective catalytic reduction of NO by $C_3H_6$ found that the catalytic performance depended on the chemical nature of copper species. As XRD indicated, in the conventionally dried catalyst a significant fraction of the nitrate precursor is still present after the activation pre-treatment so final decomposition upon heating at the beginning of the SCR experiment must lead to $Cu^{2+}$ species. In this sense, notice the apparent negative conversion peak which is also present in Cu 1.1.30.C and Mn 0.1.60.C, denoting NO formation, but which is absent in Cu 0.1.30.M. In the latest, as XRD showed, the microwaves-assisted drying, besides favouring the total nitrate decomposition during the activation step, seems to induce copper reduction to $Cu^+$ and $Cu^0$ states that could be less active for SCR reaction. In this sense, note also that when a second cycle is performed over Cu 0.1.30.C after cooling the sample in inert gas the negative peak disappears, the catalysts starts converting at lower temperature once the precursor has been decomposed, and the conversion curve becomes more similar to that of Cu 0.1.30.M. A possible explanation for the latter observation might be a change of the copper redox state during the first cycle as proposed by other authors [38].

Another result worthy of noting is the difference between the above copper catalysts (including Cu 1.1.30.C) and that containing manganese. The former are not only more active at lower temperature but the window at which they keep this activity is much wider (almost 300 °C). This is typically considered an advantage for operation under real conditions in which temperature may fluctuate much more easily than at lab-scale [3]. Our results contrast with those from other authors who have found that for the same reaction manganese oxides are more active at low temperature than copper oxides but when supported on carbon/ceramic monoliths [31] or prepared by precipitation methods [39]. Our manganese catalyst exhibits also poorer performance if compared to the $Mn_2O_3$ reported in [40] but in that study pitch-based active carbon fibers, to which extraordinarily capacity to disperse the metal-oxide particles and create large gas-contact surface area is attributed, were used as support. Also interesting and in agreement with the other characterisation results, the pre-treatment of the support with acid before the metal impregnation does not affect significantly the catalytic performance (observe the similarity of the conversion profiles obtained for the Cu 0.1.30.C and Cu 1.1.30.C catalysts). The apparent lower activity of Cu 1.1.30.M respect Cu 0.1.30.M should be associated with the fact that for this catalyst the tested monolith weight was lower (see W/F in Table 3) indicating that the microwave drying might be more aggressive after the acid treatment removing part of the carbon. The similar shape of the catalytic profiles for both samples suggests that the nature of the active phase sites does not change but its number is lower in the Cu 1.1.30.M catalysts (recall that both samples presented similar metal/carbon ratio, Table 1). Finally, notice that the catalytic behaviour of Cu int is clearly poorer in good accordance with the rest of characterisation results which suggested that in this sample much less Cu must be accessible on the catalyst surface as consequence of the preparation method. Also as expected, the monolith support without metal shows the worst performance among the samples investigated. Whatever the influence of the other elements than Cu or Mn present in the catalysts may be (recall EDS data), what this blank experiment suggests is that their contribution cannot be considered significant as only low activity at the highest range of temperature studied is observed.

## 4. Conclusions

In this work the influence of the preparation method on copper- or manganese-supported carbon-based honeycomb monoliths has been studied as a previous necessary step before their use at lab-scale for the selective catalytic reduction of NO using ammonia as reducing agent. The combined used of standard complementary techniques has allowed to understand the origin of the significant differences shown by the catalysts depending on their preparation procedure, both in their physico-chemical properties and catalytic activity.

The most relevant result is related to the use of microwaves for impregnated monoliths drying which leads to a better metal distribution and level of dispersion as compared with conventional drying methods. Moreover, the unusual application of Rietveld analysis for the X-ray diffraction results has allowed detecting also differences in the phases formed as a consequence of the way of drying. Also remarkable, simple metal activation by heating the monoliths under inert gas at 250 °C after impregnation can be insufficient to decompose fully the metal precursor in samples submitted to conventional drying. This result also demonstrates that extrapolation of conclusions related to metal activation procedures from powders to monolithic catalysts should be taken with care.

Regarding the way of introducing the metal phase, the most significant results is that integration of the metal precursor before extrusion does have noticeable implications like more difficulty to activate the carbon support without causing undesirable effects on the metal or its reaction with the additives employed for the monolith extrusion. In relation with the Mn catalysts, after same drying conditions, manganese precursor seems to decompose

more easily and spread better than that of copper over the monolithic carbon support.

Finally, the catalytic tests in the SCR of NO with $NH_3$ have provided results which are consistent with those derived from the characterisation techniques like the advantaged behaviour of impregnated monoliths regarding the integral one and the differences between catalysts dried conventionally and employing microwaves. Nonetheless, the most significant outcome has been that the influence of the drying method in the final redox state of the metal and therefore on the nature of the active sites can be more critical than the effect on the metal phase distribution. This might also explain the differences between copper and manganese-impregnated catalysts. Also remarkable, some of the Cu catalyst investigated exhibit a very high activity at low temperature which is in addition stable in a wide temperature window, upon consecutive cycles and with time, rendering the less explored in literature carbon-supported copper catalysts an attractive formulation for NO-SCR.

The above results are of interest in the context of testing carbon-based honeycomb monoliths as metal support for catalytic applications at industrial scale.

## Acknowledgements

This work has been funded by the AM17/04 and A/4870/06 Projects of the Junta de Andalucía and AECI (Spain), respectively. The authors thank the Central Services of Science and Technology of the UCA for the use of their facilities and S. Zerrad and P. Yeste, both members of the Solid State Chemistry and Catalysis UCA research group, for their help with the TGA experiments. They also acknowledge the remarks from referees and editor which have helped to improve the manuscript.

## References

[1] H. Marsh, Activated Carbon Compendium, first ed., Elsevier, Oxford, UK, 2001.
[2] A.B. Stiles, Catalyst Supports and Supported Catalysts, Butterworths, Stoneham, MA, USA, 1987.
[3] R.M. Heck, R.J. Farrauto, S.T. Gulati, Catalytic Air Pollution Control: Commercial Technology, second ed., Wiley, New York, 2002.
[4] A. Cybulski, J.A. Moulijn, Structured Catalysts and Reactors, Marcel Dekker, Inc., New York, USA, 1998.
[5] J. Benbow, J. Bridgwater, Paste Flow and Extrusion, Clarendon Press, Oxford, UK, 1993.
[6] J.M. Rodríguez-Izquierdo, H. Vidal, J.M. Gatica, D. Sánchez, A.M. Cordón, ES Patent 2221782 B1, University of Cádiz, Spain, 2005.
[7] J.M. Gatica, J.M. Rodríguez-Izquierdo, D. Sánchez, C.O. Ania, J.B. Parra, H. Vidal, Carbon 42 (2004) 3251–3254.
[8] J.M. Gatica, J.M. Rodríguez-Izquierdo, D. Sánchez, T. Chafik, S. Harti, H. Zaitan, H. Vidal, C.R. Chimie 9 (2006) 1215–1220.
[9] R.M. Heck, S. Gulati, R.J. Farrauto, Chem. Eng. J. 82 (2001) 149–156.
[10] V. Tomasic, Catal. Today 119 (2007) 106–113.
[11] B. Huang, R. Huang, D. Jin, D. Ye, Catal. Today 126 (2007) 279–283, and references thereof cited.
[12] G. Marbán, T. Valdés-Solís, A.B. Fuertes, J. Catal. 226 (2004) 138–155.
[13] G. Leofanti, G. Tozzola, M. Padovan, G. Petrini, S. Bordita, A. Zecchina, Catal. Today 34 (1997) 329–352.
[14] G. Mul, J.A. Moulijn, Supported Metals in Catalysis, Catalytic Science Series, 5, Imperial College Press, London, 2005.
[15] T. Vergunst, M.J.G. Linders, F. Kapteijn, J.A. Moulijn, Catal. Rev. 43 (3) (2001) 291–314.
[16] S. Wang, G.Q. Lu, Carbon 36 (3) (1998) 283–292.
[17] T. Vergunst, F. Kapteijn, J.A. Moulijn, Appl. Catal. A 213 (2001) 179–187.
[18] A. Wahlberg, L.J. Pettersson, K. Bruce, M. Andersson, K. Jansson, Appl. Catal. B 23 (1999) 271–281.
[19] E. Gippini, Pastas Cerámicas, Sociedad Española de Cerámica, Madrid, Spain, 1979
[20] J.J. Rodríguez-Carvajal, Phys. B, Condens. Matter 192 (1993) 55–69.
[21] A. Bahamonde, F. Mohino, M. Rebollar, M. Yates, P. Avila, S. Mendioroz, Catal. Today 69 (2001) 233–239.
[22] F. Mohino, P. Avila, P. Salerno, A. Bahamonde, S. Mendioroz, Catal. Today 107/108 (2005) 192–199.
[23] J.C. Martin, P. Avila, S. Suárez, M. Yates, A.B. Martín-Rojo, C. Barthelemy, J.A. Martín, Appl. Catal. B 67 (2006) 270–278.
[24] F.J. Williams, N. Malikova, R.M. Lambert, Catal. Lett. 90 (3/4) (2003) 177–180.
[25] W.H. Qi, M.P. Wang, J. Nanoparticle Res. 7 (2005) 51–57.
[26] G. Fierro, M. Lo Jacono, M. Inversi, P. Porta, R. Lavecchia, F. Cioci, J. Catal. 148 (1994) 709–721.
[27] G. Qi, R.T. Yang, J. Catal. 217 (2003) 434–441.
[28] O. Kröcher, M. Devadas, M. Elsener, A. Wokaun, N. Söger, M. Pfeifer, Y. Demel, L. Mussmann, Appl. Catal. B 66 (2006) 208–216.
[29] S. Bennici, A. Gervasini, N. Ravasio, F. Zaccheria, J. Phys. Chem. B 107 (2003) 5168–5176.
[30] J.A. Sullivan, Catal. Lett. 79 (1–4) (2002) 59–62.
[31] X. Tang, J. Hao, H. Yi, J. Li, Catal. Today 126 (2007) 406–411.
[32] M. Brandhorst, J. Zajac, D.J. Jones, J. Rozière, M. Womes, A. Jiménez-López, E. Rodríguez-Castellón, Appl. Catal. B 55 (2005) 267–276.
[33] L. Chmielarz, P. Kuśtrowski, R. Dziembaj, P. Cool, E.F. Vansant, Catal. Today 119 (2007) 181–186.
[34] S. Bennici, A. Gervasini, M. Lazzarin, V. Ragaini, Ultrason. Sonochem. 12 (2005) 307–312.
[35] B. Huang, R. Huang, D. Jin, D. Ye, Catal. Today 126 (2007) 279–283.
[36] M.C. Kung, H.H. Kung, Top. Catal. 28 (1–4) (2004) 105–110.
[37] Q. Lin, J. Hao, J. Li, Z. Ma, W. Lin, Catal. Today 126 (2007) 351–358.
[38] D. Liu, H.J. Robota, J. Phys. Chem. B 103 (1999) 2755–2765.
[39] M. Kang, E.D. Park, J.M. Kim, J.E. Yie, Appl. Catal. A 327 (2007) 261–269.
[40] M. Yoshikawa, A. Yasutake, I. Mochida, Appl. Catal. A 173 (1998) 239–245.